Elasticity and Phase Behavior of Nematic Elastomers

M. Warner* and X. J. Wang†

Cavendish Laboratory, Madingley Road, Cambridge CB3 0HE, England

Received December 19, 1990; Revised Manuscript Received March 21, 1991

ABSTRACT: We describe the molecular basis of unusual phenomena displayed by nematic networks including phase transitions, spontaneous shape changes, discontinuous stress–strain relations, and nonlinear stress–optical laws. Such rubbers are composed of polymer chains of stiff rods either linked by flexible spacers to form a backbone polymer or, in the case of comb polymers, linked as pendants. We describe the polymers as wormlike chains in a nematic field. We also calculate deviations from classical behavior of conventional (nonnematic) elastomers due to residual nematic interactions.

1. Introduction

A nematic elastomer represents the confluence of long-chain elasticity and nematic order which, when combined, give solids exhibiting unusual phenomena such as spontaneous shape changes, (ideally) discontinuous stress–strain relations, and strong deviations from classical behavior when in their nonnematic phase. Thus, in addition to describing the new phenomena found in nematic rubbers, our investigations suggest why deviations from the classical stress–strain relation are found in conventional, that is, nonnematic, elastomers. We shall propose, as others have done, that residual nematic interactions are responsible for those deviations.

Initially de Gennes[1,2] recognized that while stress must be applied to a classical polymer network to cause molecular shape changes, nematic polymers in a melt spontaneously change their shape as they orient. Thus, nematogenic polymers cross-linked into a network could allow mechanical effects (stress and strain) to couple to nematic (orientational) order and vice versa. de Gennes[1,2] predicted unusual consequences such as mechanically induced nematic phase transitions, discontinuous stress–strain relations with associated mechanical critical points, and solids exhibiting spontaneous shape changes. In a series of beautiful experiments that overcome the masking effect of polydomains, Schätzle et al.[3] have seen these effects.

The molecular theory of nematic networks was developed by Warner et al.[4] (WGV) and Khokhlov et al.,[5a-c] in ways differing slightly in the microscopic description of chains: In a conventional network when a chain is distorted by applied stress from its natural shape, the free energy rises largely because this new constraint lowers the entropy. When a network becomes nematic, its chains change their natural shape away from spherical. If the network could then change its shape so that its nematic chains could adopt their natural aspherical shape, there would be no additional elastic rise to the free energy. Unfortunately, chains are constrained by their attachment to the network. In particular, the incompressibility of rubbers, when dealing with rubber elasticity, means that chains must change shape while conserving volume. It turns out that a change of chain shape to the one natural in the melt violates this requirement and is unattainable. Thus, in a nematic network chains are further distorted from their natural shape and elastic free energy rises. This is easily calculated[4] for anisotropic Gaussian chains, that is, polymers long enough to be distorted random walks[6,7] rather than rodlike when in the nematic state.

† Permanent address: Department of Physics, Tsinghua University, Beijing, China.

The concept of nematic interactions helping to distort chain shapes was also the basis of many phenomenological descriptions of the deviations of conventional elastomers away from classical theory.[8-11] This concept was also recognized to be involved in conventional networks by Abramchuk and Khokhlov.[5] As all these authors[5,8-11] and WGV[4] point out, when nematic interactions are present, chain free energy (even in a purely Gaussian network, such as that described later by eq 10) is no longer purely a question of entropy. There is an energetic component which is a function of the degree of alignment whether this is achieved by applied stress or is spontaneous. The work of ref 5, while being motivated in the same way as this work, relies on a rather different model of chains, the differences being discussed below. We shall proceed with the method of WGV,[4] commenting later on ref 5 and on phenomenological approaches.[8-11]

The spontaneous distortion $\lambda_m(Q)$ of a nematic monodomain rubber (Q is the nematic order parameter) depends on the chain shape in the aligned state. If l_z and l_p are the effective step lengths of the chain, respectively parallel and perpendicular to the ordering direction, WGV,[4] then $\lambda_m = (l_z/l_p)^{1/3}$. Clearly when both step lengths take the isotropic value l_0, then there is no distortion, i.e., $\lambda = 1$. l_z and l_p are functions of Q for semiflexible chains,[6] the results being quoted in the next section. These were used by WGV,[4] and we shall develop that model instead of the freely jointed chain model.[5]

λ_m is the distortion that minimizes the additional elastic free energy. An elastic addition to the nematic free energy implies that isotropic–nematic phase transitions must be depressed by cross-linking. Within perturbation theory[4] in Q a term in $+Q^4$ is added to the free energy. As de Gennes first described, cross-linking in the nematic state[1] freezes in a memory of order and enhances the stability of the nematic. WGV[4] derived the extra $-Q_x^2Q^2$ term (Q_x is the order at cross-linking) in the free energy which elevates the transition temperature, the case that had interested de Gennes.[1,2]

A shape change λ implies work (per unit volume) of $-\sigma \ln \lambda$ is done on a sample held at constant true stress σ. Since $\lambda(Q)$ is known, one can construct a microscopic theory of how applied mechanical stress couples, via shape $\lambda(Q)$ to the nematic order, Q. Thus, the nematic, elastic, and external energies are available. Full numerical solutions of the resulting equations for phases, stress–strain relations, rubber modulus, and stress–optical (order parameter) effects will be presented.

In the paranematic state, that is, above the phase transition but with an external field applied, the order can be small and a perturbative approach appropriate.

0024-9297/91/2224-4932$02.50/0

The perturbative method can describe the approach to the nematic state where incipient nematic tendencies mean that there will be strong deviations from the stress–optical law. Another application is to describe deviations from classical behavior in nonnematic (conventional) rubbers where the nematic state is fictious since it is at unattainably low temperatures. There are, however, residual nematic interactions of steric and van der Waals origin. Thus, elasticity is not purely entropic, the energetic component being dependent on alignment.[5a-c,11]

We shall present a sketch of the underlying theory and then full numerical and perturbative results for the various effects described above. This model is equally applicable to main-chain (MC) or side-chain (SC) polymers. MC polymers are simpler to visualize. The nematic order Q is $Q = \langle P_2(\cos\theta)\rangle = \langle {}^3/_2 \cos^2\theta - {}^1/_2\rangle$, where $\theta(s)$ is the angle the tangent vector of the chain (at arc position s along the chain) makes with the ordering direction (the director), here z. Q must be positive for a stable nematic phase. Spontaneous orientation or the application of extensional stress extends the chain to a prolate shape: $\langle R_z^2\rangle = {}^1/_3 l_z(Q)L$, $\langle \mathbf{R}_p^2\rangle = {}^2/_3 l_p(Q)L$ with $l_p < l_0 < l_z$ and L the total arc length of a chain. SC possibilities are more complex since one can envisage[12] two components, the backbone and side chains, with order parameters Q_B and Q_A, respectively. At least one of these must be positive to have a stable phase; whence, there are three possible uniaxial nematic phases: N_I, N_{II}, N_{III}. The latter two have $Q_B > 0$; that is, the chain is still prolate. Since elasticity depends on the shape of the backbone, these phases are qualitatively like a MC system, albeit with modified values of Q_B at a transition. N_I is naturally oblate, $Q_B < 0$, whence $l_z < l_0 < l_p$ and $\lambda_m < 1$. A monodomain of a nematic rubber with this symmetry flattens. This last case with $Q < 0$ has the same symmetry as a MC system with an orientation induced by compressional stress.

Experiments on nematic elastomers have been performed on both SC[3,13,14] and MC[15] systems but always, to our knowledge, on prolate phases to which we shall restrict ourselves here.

2. Theory

2.1. Brief Description of Chain Statistics. As outlined above, to model a naturally anisotropic network, one must find the natural shape of a chain when an order Q is present. Liquid crystal polymers are described by spheroidal wave functions[6,16-18] appropriate to wormlike chains oriented by a nematic mean field which couples to the local chain direction. Worm polymers, with bend constant ϵ, in a nematic mean field of strength $v_b Q$ have a Hamiltonian[16] H:

$$H[\mathbf{u}(s)] = {}^1/_2\epsilon\int_0^L \left|\frac{d\mathbf{u}}{ds}\right|^2 ds - v_b Q\int_0^L P_2(\cos\theta)\, ds \quad (1)$$

The unit vector $\mathbf{u}(s)$ is the tangent vector of the chain at contour point s. The first term penalizes bend. v_b is the nematic coupling constant. The combination $Qv_bP_2(\cos\theta)$ is the nematic mean field.[19] The partition function Z is then the sum over all configurations of the corresponding Boltzmann factor, with $\beta = 1/k_BT$:

$$Z = \int \delta\mathbf{u}(s)\, \exp\{-\beta H[\mathbf{u}(s)]\} \quad (2)$$

For a uniaxial phase eq 2 is equivalent to a spheroidal wave equation of zero rank for eigenfunctions $Sp_{0n}(\theta)$ and eigenvalues $(\lambda_{0n} - {}^2/_3\Delta^2)$.

$$\left[(\lambda_{0n} - {}^2/_3\Delta^2) + D\frac{1}{\sin\theta}\frac{d}{d\theta}\left(\sin\theta\frac{d}{d\theta}\right) + \Delta^2(1-\cos^2\theta)\right]Sp_{0n}(\theta) = 0 \quad (3)$$

D is $1/(2\beta\epsilon)$, the inverse of which, D^{-1}, is the persistence length of the free worm, also denoted by l_0 below. The effective coupling is $\Delta^2 = -3Q/\tilde{T}^2$ with the reduced temperature being $\tilde{T} = k_BT/(v_b\epsilon)^{1/2}$. The energy scale in this problem is thus the geometric mean of the nematic and bend energies. Equation 3 is a rotational diffusion equation, with rotational diffusion constant D, and represents the wandering of the tangent over the surface of the unit sphere of directions as one evolves in arc position along the chain. To see the equivalence of (2) to (3), one constructs the propagator $G(\theta,\theta';s,s')$

$$G(\theta,\theta';s,s') = \sum_{n=0}^{\infty} Sp_{0n}(\theta)Sp_{0n}(\theta')\exp[-\lambda_{0n}D|s-s'|] \quad (4)$$

which is the joint probability of the chain having angle θ' at arc point s' and angle θ at s. The partition function is $Z = \int d(\cos\theta)\, d(\cos\theta')G(\theta,\theta';L,0)$. For very long chains the ground state dominates the higher excited states and $Z \sim \exp(-\lambda_{00}LD)$. Since $F = -k_BT\ln Z$, the ground-state eigenvalue λ_{00} is part of the free energy of one persistence length of a long chain.

It will be useful to expand various quantities in a series for small coupling Δ^2. The expansion of λ_{00} in Δ^2 is given in ref 6. The expansion of other eigenvalues and of the eigenfunctions Sp_{ml} may be found in the paper Bouwkamp.[20] The Sp_{ml} values are expanded as a series in Legendre polynomials of the same symmetry.

The order parameter Q for a long chain is given by the matrix element

$$Q = \langle Sp_{00}(\theta)|P_2(\cos\theta)|Sp_{00}(\theta)\rangle \quad (5)$$

which is what survives when G is used to average P_2 (see ref 6).

The effective step lengths parallel and perpendicular to the director emerge from similar averages (using G) of the square dimensions $\langle R_z^2\rangle$ and $\langle \mathbf{R}_p^2\rangle$:

$$\frac{3\langle R_z^2\rangle}{l_0L} = \frac{l_z}{l_0} = \frac{3}{2}\sum_{n=0}^{\infty}\frac{2n+1}{\lambda_{0n}-\lambda_{00}}(\langle Sp_{0n}(\theta)|P_1(\cos\theta)|Sp_{00}(\theta)\rangle)^2$$

$$\frac{3}{2}\frac{\langle \mathbf{R}_p^2\rangle}{l_0L} = \frac{l_p}{l_0} = \frac{3}{4}\sum_{n=1}^{\infty}\frac{1}{\lambda_{1n}-\lambda_{00}}\frac{2n+1}{n(n+1)}(\langle Sp_{1n}(\theta)\times |P_{11}(\cos\theta)|Sp_{00}(\theta)\rangle)^2 \quad (6)$$

The Sp_{1n}'s are the first-rank spheroidal wave functions; P_1 and P_{11} are the Legendre functions. Expanding eigenfunctions and eigenvalues perturbatively yields expansions for the l

$$\frac{l_z}{l_0} = 1 - \frac{2}{9}\Delta^2 + \frac{4}{3^3\cdot 5}\Delta^4 + O(\Delta^6) \equiv 1 + aQ + bQ^2 + O(Q^3)$$

$$\frac{l_p}{l_0} = 1 + \frac{1}{9}\Delta^2 + O(\Delta^6) \equiv 1 - \frac{a}{2}Q + O(Q^3) \quad (7)$$

where $a = 2/(3\tilde{T}^2)$ and $b = 4/(15\tilde{T}^4)$. There is a misprint in eq 9 of WGV;[4] the equations should be $l_0/l_z = 1 + 2\Delta^2/9 + 8\Delta^4/(3^4\cdot 5) = 1 - aQ + (a^2 - b)Q^2$ and $l_0/l_p = 1 - \Delta^2/9$

$+ \Delta^4/81 = 1 + aQ/2 + a^2Q^2/4$. Here is quoted the reciprocal of what is quoted there.

The free energy per persistence length of chain F/LD is[6]

$$F/(LDk_BT) = \lambda_{00} + Q^2/\tilde{T}^2 \quad (8)$$

$$F/(LDk_BT) = {}^1/_2AQ^2 - {}^1/_3BQ^3 + {}^1/_4CQ^4 \quad (9)$$

where the second term in (8) is the usual correction in mean field theory to avoid double counting. Equation 9 reconstructs the Landau–de Gennes form of the free energy, first derived from the spheroidal picture by Rusakov and Shliomis.[17] The coefficients arise from the perturbation expansion of λ_{00}: $A = 2(\tilde{T}^2 - 2/15)/\tilde{T}^4 \equiv A_0(\tilde{T} - \tilde{T}^*)$ with $A_0 = 2[\tilde{T} + (2/15)^{1/2}]/\tilde{T}^4$ being roughly constant for $\tilde{T}$ around the transition and with $\tilde{T}^* = (2/15)^{1/2}$, $B = 4/(3{\cdot}5{\cdot}7)/\tilde{T}^6$, and $C = 104/(3^3{\cdot}5^3{\cdot}7)/\tilde{T}^8$. $\tilde{T}^*$ is the pseudo-second-order transition temperature, and the approach of $\tilde{T}$ to $\tilde{T}^*$ in the A term is the principal temperature variation in the problem. The transition temperature is, within the Landau–de Gennes picture, $\tilde{T}_{ni} = \tilde{T}^* + (2/9)(B^2/A_0C) = \tilde{T}^* + 0.10 = 0.465$. The addition of 0.10 arises by assuming $\tilde{T} = \tilde{T}^*$ in the estimation of A_0, B, and C. The discrepancy between this result and the result of the numerical calculation[6] from (8), $\tilde{T}_{ni} = 0.388$, is due to the neglect within the Landau theory of higher terms in Q.

We use either the full form (8) in numerical results or the expanded form (9), with coefficients given by microscopic theory, in perturbation analysis. The former is vital for properties of elastomers in the nematic phase and for phase transitions since Q is generally large. The latter describes the paranematic state and explores corrections to classical elasticity theory steming from residual nematic interactions. The free energy of the underlying nematic phase and the shapes natural to chains in it are what is required for nematic networks which are now described.

2.2. Sketch of a Microscopic Theory of Nematic Networks. 2.2.1. Elastic Free Energy. The free energy shift of a nematic chain derives from the probability of **R**, the end to end vector of a strand, that is the chain between cross-links

$$P(\mathbf{R}) = (2\pi l_0 L)^{-3/2}\left(\frac{l_0^3}{l_z l_p^2}\right)^{1/2} \exp\left[-\left(\frac{3R_z^2}{2l_zL} + \frac{3\mathbf{R}_p^2}{2l_pL}\right)\right] \quad (10)$$

where R_z and $\mathbf{R}_p$ are components of **R** parallel and perpendicular to the director. We assume here that the chain is long enough that, even when in the distorted state, it remains essentially Gaussian, albeit an anisotropic Gaussian. The mean square end to end distances under this assumption can be read off (10): $\langle R_z^2\rangle = l_zL/3$ and $\langle \mathbf{R}_p^2\rangle = 2l_pL/3$, with l_z and l_p given in terms of the nematic order Q as discussed above and L being the chain arc length between cross-links.

After cross-linking, the usual assumption is made that cross-link positions affinely deform with the bulk deformation λ because of the constraint of the cross-links. Thus, a chain's end to end vector deforms from $\mathbf{R}_0$ to $\mathbf{R} = \lambda\mathbf{R}_0$, where λ is a symmetrical rank 2 tensor. In fact, fluctuations make the affine assumption invalid, a result well-known in the literature on nonnematic networks. In nematic networks WGV[4] show that these effects are present in precisely the same way; for instance, the prefactor becomes $(1 - 2/\varphi)$, where φ is the cross-link functionality. However, the nematic aspects of the problem are not materially affected.[4] For uniaxial deformations there are only two distinct principal extension ratios, λ_z and λ_p, and because of the incompressibility of rubbers, they satisfy the relation $\lambda_z\lambda_p^2 = 1$. Accordingly, the additional elastic free energy of a strand of the network with the deformed span **R** is given by

$$F_{el} = -k_BT\langle \ln P(\mathbf{R})\rangle_{P_0} \quad (11)$$

where P_0 is the probability at $\mathbf{R}_0$ at cross-linking. If the chains are cross-linked in the isotropic state, P_0 is an isotropic Gaussian, that is, (10) with l_z and l_p set equal to l_0. Taking logs and averaging, one obtains for one strand, denoting λ_z by λ (whence by incompressibility λ_p is $\lambda^{-1/2}$)

$$\frac{F_{el}(\lambda)}{k_BT} = \frac{1}{2}\left(\lambda^2\frac{l_0}{l_z} + \frac{2}{\lambda}\frac{l_0}{l_p}\right) - \frac{1}{2}\ln\left(\frac{l_0^3}{l_z l_p^2}\right) \quad (12)$$

Detailed results are presented only for systems cross-linked in the isotropic state. Reference 4 gives the microscopic picture of how cross-linking in the nematic state elevates the phase transition in the network. There are definite advantages to cross-linking in the nematic state: Legge et al.[13] have shown that one can obtain monodomain samples, memory of this state being retained after excursions into the isotropic phase.

When an external true stress σ is applied along the director, our z axis in Cartesian coordinates, it causes an additional elastic free energy per unit volume.

$$F_{ext}(\lambda,\sigma) = -\sigma \ln \lambda \quad (13)$$

Adding up the three contributions yields the total free energy $\tilde{F}$ per unit volume.

$$\tilde{F}/k_BT = N_sLD\left(\lambda_{00} + \frac{Q^2}{\tilde{T}_2}\right) + \frac{1}{2}N_s\left[\left(\lambda^2\frac{l_0}{l_z} + \frac{2}{\lambda}\frac{l_0}{l_p}\right) - \frac{1}{2}\ln\left(\frac{l_0^3}{l_z l_p^2}\right)\right] - \frac{\sigma}{k_BT}\ln\lambda \quad (14)$$

The number density of strands is $N_s = 1/(LDv_p)$, where v_p is the volume of a persistence length.

The total free energy thus comprises three contributions: the nematic contribution F_{nem}, either eq 8 or eq 9, the elastic part, eq 12, and the external work $F_{ext}(\lambda,\sigma)$, (13). It is a function of Q and λ, coupled through the elastic term, where λ appears explicitly and Q implicitly in the l_z,l_p factors.

2.2.2. Distortions of the Networks. The optimum extension λ at a given Q should minimize the free energy. Setting the partial derivative of the total free energy with respect to λ equal to 0, one obtains a condition for the equilibrium extension:

$$\frac{\sigma}{N_sk_BT} = \lambda^2\frac{l_0}{l_z} - \frac{1}{\lambda}\frac{l_0}{l_p} \quad (15)$$

The spontaneous extension λ_m is given by the solution of (15) with $\sigma = 0$.

$$\lambda_m = (l_z/l_p)^{1/3} \quad (16)$$

It is a function of chain shape, as defined by l_z and l_p, and hence a combination of the order parameter Q and the reduced temperature $\tilde{T}$, that is, of the coupling $\Delta^2 = -3Q/\tilde{T}^2$. Note that in a network the chain extension in the z direction is forced to differ from the natural extension which would be $(l_z/l_0)^{1/2}$, and hence the free energy rises. When λ_m is inserted into (12), the stress-free elastic free

energy at the minimizing extension is

$$F_{el} = {}^3/_2 k_B T(W - \ln W) \tag{17}$$

where $W = (l_0^3/l_z l_p^2)^{1/3}$ is a function of Δ^2 and hence Q and is important below.

Perturbation theory, eq 7 for l_z and l_p, gives λ_m as a series in Q and in eq 17 yields additions to the Landau–de Gennes free energy: $+Q^4$ for cross-linking in the isotropic state and $+Q^4$ plus an additional term $-Q^2$ for cross-linking in the nematic state.[4] The nematic–isotropic (N–I) transition temperature $\tilde{T}_{ni}$ then shifts down or up, respectively, through additions to A_0 or C factors. The effect on Landau descriptions of the network has been given in ref 4.

Nematogenic networks, like any rubber, resist stress. The reduced stress is denoted by $\sigma^* = \sigma/N_s k_B T$. Extracting a factor of $\lambda_m(Q)$ from λ, $\lambda = \lambda_m t$, the stress–strain relation 15 becomes an equation for $t(Q,\sigma^*)$

$$t^3 - (\sigma^*/W)t - 1 = 0 \tag{18}$$

where t is clearly a function only of the combination σ^*/W. Setting $(4/27)(\sigma^*/W)^3 = \alpha$, the cubic eq 18 has elementary solutions. If stress is great or the temperature low, or the cross-link density low enough, then $\alpha > 1$ and there are three real roots. Two of them are discarded on physical grounds, the last one is $t = 2^{2/3}\alpha^{1/2}\cos[\cos^{-1}(\alpha^{-3/2})/3]$, a result exploited in the numerical analysis. If $\alpha \leq 1$, the equation has only one real root, namely $t = 2^{-1/3}\{[1 + (1 - \alpha)^{1/2}]^{1/3} + [1 - (1 - \alpha)^{1/2}]^{1/3}\}$.

Now strain $\lambda = \lambda_m(Q)t(\sigma^*/W(Q))$ has been related to stress σ^* and the order parameter Q. However, Q is still unknown and must be fixed before we have the final relation between λ and σ^* and the full free energy.

2.2.3. Order of the Network. The order parameter, $\langle P_2(\cos\theta)\rangle$, is no longer given by the matrix element $\langle Sp_{00}|P_2(\cos\theta)|Sp_{00}\rangle$ because eq 2 and hence eq 3 and 4 are no longer sufficient to give chain probabilities. These are now also influenced by elastic contributions.

λ has been found as a function of Q. Returning this to $F_{el}(Q,\lambda(Q))$ gives a total free energy now only a function of Q. Minimizing with respect to Q defines the order parameter Q. The total derivative of free energy with respect to Q is set equal to 0.

$$\frac{dF}{dQ} \equiv \left(\frac{\partial F}{\partial Q}\right)_\lambda + \left(\frac{\partial F}{\partial \lambda}\right)_Q \left(\frac{d\lambda}{dQ}\right) = 0 \tag{19}$$

To find $\lambda(Q)$, we have already solved $(\partial F/\partial\lambda)_Q = 0$ (eq 15); under these conditions (19) reduces to

$$(\partial F/\partial Q)_\lambda = 0 \tag{20}$$

which is a self-consistency equation for Q. Equation 20 yields an expression for the order parameter Q

$$Q = \langle Sp_{00}(\theta)|P_2(\theta)|Sp_{00}(\theta)\rangle + \frac{3}{2}\frac{1}{LD}\frac{\partial}{\partial\Delta^2}\left(\frac{F_{el}}{k_B T}\right)_\lambda$$
$$\equiv f(Q,\lambda(Q)) \tag{21}$$

where the Pauli trick[6] allows the derivative dF_{nem}/dQ to be replaced by the matrix element. The first part of (21) has the same form as the counterpart nematic polymer melt. The second part is the contribution of cross-links and the external stress. It arises from the coupling of displacement and orientation. The factor of $(1/LD)$ reduces the strand free energy to a value per persistence length. Note that F_{el} depends on λ and on Q (through the Q dependence of l_z and l_p) and that λ is kept fixed in (20).

Solving (21) for Q completes the problem. Q can now be inserted in $\lambda_m(Q)$ and $t(Q,\sigma^*)$ to give the final connection between λ and σ^*. Q and $\lambda(Q)$ can be put in F_{nem} and F_{el}, and $-\sigma \ln \lambda(Q)$ to give the overall free energy and hence the phase stability predicted.

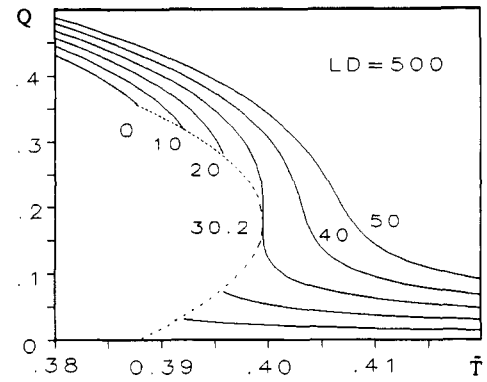

Figure 1. Order parameter Q as a function of reduced temperature $\tilde{T}$ $(=k_B T/(\upsilon_b\epsilon)^{1/2})$ for a variety of stresses σ^* $(=\sigma/N_s k_B T)$. The strand length is 500 in units of the persistence length D^{-1}.

Increasing temperature at $\sigma = 0$ induces a first-order N–I phase transition. The order parameter jumps from a finite value to zero at the transition temperature. For various applied σ^*, the dependence of Q on $\tilde{T}$ is shown in Figure 1. A first-order phase transition between higher and lower temperature phases occurs for σ^* up to a critical value σ^*_c. The former phase has nonzero Q and is a paranematic phase. As stress is increased, the phase transition moves to higher temperature—the orienting effect of stress stabilizes the nematic phase. When the stress is beyond the critical value σ^*_c, the distinction between the phases disappears. This behavior is qualitatively the same as that of simple nematics in external electric or magnetic fields and has been discussed for polymer liquid crystals by Wang and Warner.[21] Optical birefringence is proportional to the nematic order parameter. Thus, these networks exhibit stress–optical effects. Strong spontaneous nematic tendencies make such effects vastly greater than in classical networks, and we discuss them below.

2.3. Freely Jointed Rod Model of Nematic Networks. Khokhlov has recently drawn our attention to a series of his papers[5a–c] which attacked the nematic network problem using a freely jointed chain model and hence rather different forms for $l_z(Q)$ and $l_p(Q)$ to describe a random walk distorted by nematic interactions. As noted in the introduction, the underlying philosophy of ref 5a is otherwise the same as that of ref 4; that is, it hinges on (10). We cannot comment in detail on refs 5b and 5c since we can as yet only find them in Russian.

The freely jointed chain model replaces the real worm chain by one broken down into independent segments of length equal to the orientational correlation length. This can create difficulties: the length of the segments being aligned by the nematic field is implicitly a function of the nematic order and should therefore change. If one does not allow this change, then one cannot describe the unfolding of the chain as temperature is reduced, going (presumably via hairpins) to a rod at states of high nematic order.

The freely jointed rod model is, however, simpler than the worm model and has been found useful in describing nematic rubbers:[5a–c] if the segment length is l_0, then by simple geometry the projection of this bond onto the z axis and onto the x–y plane is $l_0\cos\theta$ and $l_0\sin\theta$, where θ is the angle it makes to the z axis. Considering random walks with these step lengths in the z direction and in the perpendicular plane, one obtains

$$\langle R_z^2\rangle/(Nl_0^2) = \langle \cos^2\theta\rangle \equiv {}^2/_3(Q + {}^1/_2) \qquad (22a)$$

$$\langle \mathbf{R}_p^2\rangle/(Nl_0^2) = \langle \sin^2\theta\rangle \equiv {}^2/_3(1 - Q) \qquad (22b)$$

One sees from (22a) that a drastic expansion of a chain to a rod is not possible. The advantage of this model is that chain conformations are simple functions of the order Q.

The elastic energy is obtained from the ideas of naturally anisotropic walks (eq 10 and following), inserting $L = Nl_0$ and $l_z = l_0({}^2/_3)(Q + {}^1/_2)$, $l_p = l_0({}^2/_3)(1 - Q)$. The nematic energy is now that of Maier and Saupe[19] for simple rods each with a nematic coupling $l_0\upsilon_b$. The appropriate reduced temperature is now instead $\tilde{T} = k_BT/(l_0\upsilon_b)$. The theory thus has a very different structure in its energy scales, conformational changes, and phase transitions and has been fully explored by Khokhlov et al.[5] For the high-temperature paranematic phase, the problem of strong chain expansion is not encountered. However, the claim to greater simplicity compared with the worm model is no longer sustainable; that is, eqs 22a and 22b are not significantly simpler than eqs 7.

2.4. Phenomenological Models. Jarry and Monnerie[9] and Deloche and Samulski[10,11] obtain by quite general phenomenological arguments the elastic free energy of the form (12) with perturbative expressions for the chain alignment factors l_0/l_z and l_0/l_p. Their coefficient E is our a. The coefficient F is related to $(a^2 - b)$. In fact, our microscopic calculation reveals that the coefficients of S^2 in the λ^2 and $1/\lambda$ terms are not in the relation 2:−1 nor is $F \ll E$ necessarily. These approaches also adopt a phenomenological nematic part to the free energy, within factors of ${}^1/_2$, ${}^1/_3$, ..., the same as our (9). In the most comprehensive studies involving stress–optical[10] and stress–strain[11] calculations B and F have been set equal to 0, a reasonable enough assumption since the regime of small distortion is being examined. We return to this below.

Jarry and Monnerie[9] conclude that nematic effects in the stress are negligible ($\sim 1/N$). We do not find this close enough to the nematic transition. In fact, this theory gives substantial deviations from classical behavior, as is found in refs 5a and 11. The reasons for this are demonstrated in our discussion of perturbative results below.

3. Numerical Results

In this section we present the results of numerically following through the scheme given in section 2 for finding $\lambda(Q)$, and then $Q = f(Q,\lambda(Q))$ is followed numerically. The spheroidal wave functions are expanded in a basis set of Legendre polynomials, yielding the eigenvalues, the first, λ_0, giving us part of the nematic free energy. The eigenfunctions give the matrix elements needed for the order (21) and for the shape of the chain via (6) for l_z, l_p. These are assembled to give the mean field part of the nematic free energy and the elastic free energy. In the nematic state, Q is always greater than certain value because the nematic network is a first-order system. Thus, for phase transitions it is never strictly legitimate to use perturbative approaches.

3.1. Stress-Free Networks. The dependence of Q on temperature T at $\sigma = 0$ is shown in Figure 2, where the scale of the transverse axis is the normalized temperature $\tilde{T} = k_BT/(\upsilon_b\epsilon)^{1/2}$. Chains with very long distances between cross-links are little constrained by the network and reproduce melt results. It is worth pointing out that there are two accidental crossing points of the network and free nematic polymer curves due to the features of W. One of them is due to $W = 1$; the other is where $dW/dQ = 0$. We

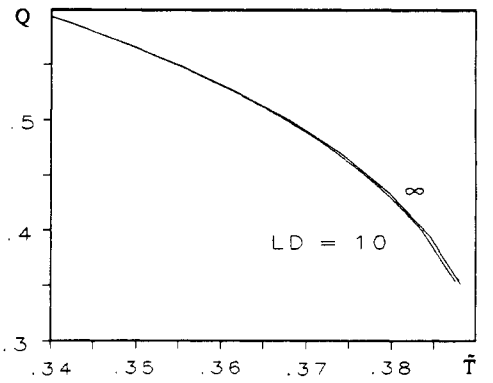

Figure 2. Dependence of order parameter Q on normalized temperature $\tilde{T}$ for stand length $LD = 10$ and infinite free polymer chain in the normal nematic temperature range while in the absence of external stress.

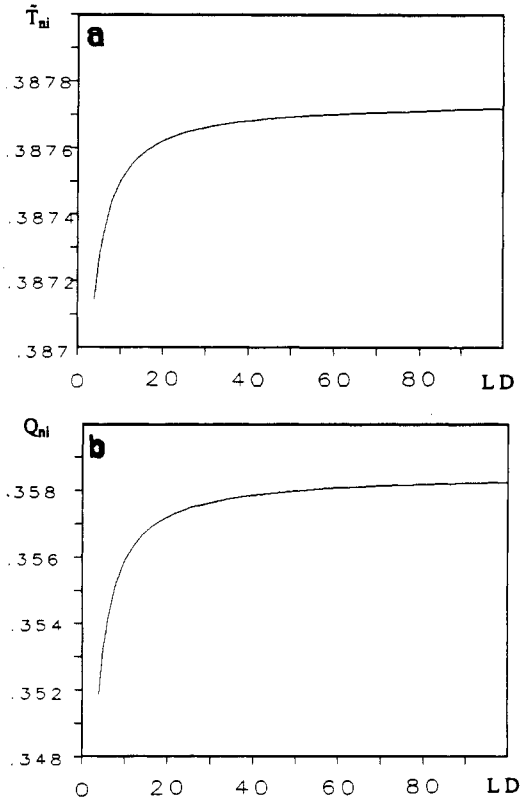

Figure 3. N–I transition temperature $\tilde{T}_{ni}$ (a) and transition order parameter Q_{ni} (b) as functions of LD.

note that in their experiments Legge et al.[13] indeed found the two crossing points when they dealt with a side-chain system. The elastically driven N–I transition temperature shifts with respect to the counterpart nematic polymer are not very remarkable. This is because the difference between the natural shape of nematic polymers and the constrained shape of strands in network, given by $W^{-1/2}$, is not significant around the transition.

Figure 3 gives the dependence of a stress-free network transition temperature on strand length measured in units of the persistence length D^{-1}. For shorter strands or higher density of cross-links the N–I transition occurs at lower temperature, the shifts from the melt being small. The associated shift in the order parameter Q is also small. The reduced transition temperature and the transition order, $\tilde{T}_{ni}$ and Q_{ni}, approach the limiting value of the melt when the strand length becomes greater than about 15 persistence lengths.

Figure 4 is the spontaneous distortion λ_m that a ne-

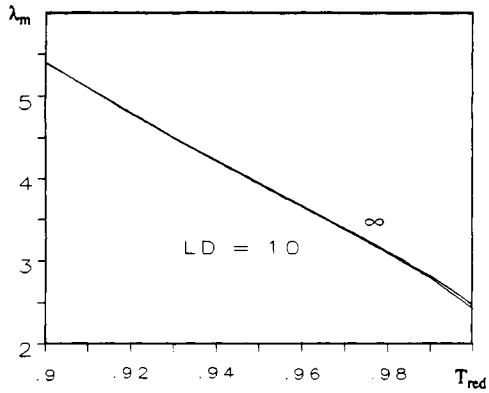

Figure 4. Spontaneous deformation of a stress-free network, λ_m, as a function of reduced temperature, T/T_{ni}. Two curves for strand length LD = 10 and infinite free polymer chain almost coincide.

matic monodomain at $\sigma = 0$ would exhibit as a function of reduced temperature $T_{red} = T/T_{ni}$. $\lambda_m = 2.46$, the extension ratio at the N-I transition for long strands, is another universal value of this theory, just like the transition order parameter $Q_{ni} = 0.356$, obtaining for strand lengths $LD \geq 15$. This universal prediction of λ_m is for main-chain PLCs and hence cannot be directly compared with the experiments of Schätzle et al.[3] and Legge et al.,[13] who used side-chain systems (albeit with the prolate symmetry associated with main-chain systems). Both papers have sophisticated methods of estimating $\lambda_m(T_{ni})$. Schätzle et al. find that creation of a monodomain is first achieved at a finite applied stress. By extrapolating back their $\lambda - \sigma$ curves to $\sigma = 0$, they estimate λ_m. Legge et al. cross-link in a monodomain sample of the nematic phase. This case is treated in ref 4.

3.2. Stressed Networks. At a fixed $\tilde{T}$ on Figure 1 one can see how Q varies with σ^* (see Figure 5), where $Q(\sigma^*)$ is shown for LD = 20 and T/T_{ni} = 0.99, 1.01, 1.02, 1.03, 1.05, and 1.5. The critical point is $\sigma^*_c = 1.2$ for LD = 20. For LD = 500 σ^*_c is 30.2; the ratio σ^*_c/LD is very insensitive to LD. Figure 5 partly summarizes the remarkable properties of nematic networks. At temperatures below T_{ni} (e.g., 0.99) the network spontaneously orders and applied stress has a less dramatic effect in inducing further order. Just above T_{ni} there is, for small σ^*, a smooth increase in Q with σ^* (see Figure 5b for a magnification of the scale). Stress is capable of inducing a phase transition, and the order jumps to a higher value discontinuously (curves 1.01, 1.02, and 1.03, the latter near the critical point). At high temperatures nematic effects are weaker and the effect of σ^* is again less dramatic.

Consulting Figure 1, below the critical stress σ^*_c the nematic and paranematic phase transition is still of first order, but in the paranematic phase the chains have some order induced by stress. For stresses beyond σ^*_c, the phase gap vanishes. The boundary of the coexistence region in Figure 1 where LD = 500 is a parabolic curve typical of mean field theory[22]

$$(Q_N - Q_P)^2 = -10.78(\tilde{T}_{ni} - \tilde{T}_c) \qquad (23)$$

where Q_N and Q_P are the nematic and paranematic values at the transition, respectively. The rise in $\tilde{T}_{ni}$ with σ^* is linear and is terminated at the critical point σ^*_c

$$\tilde{T}_{ni}(\sigma^*) = \tilde{T}_{ni}(\sigma^*=0) + 3.955 \times 10^{-4}\sigma^* \qquad (24)$$

where the stress-free value is $\tilde{T}_{ni}(\sigma^*=0) = 0.38774$ and $\tilde{T}_{ni}(\sigma^*=\sigma^*_c) = \tilde{T}_c = 0.39965$. An analogous critical point for a nematic polymer in an applied electric field was found

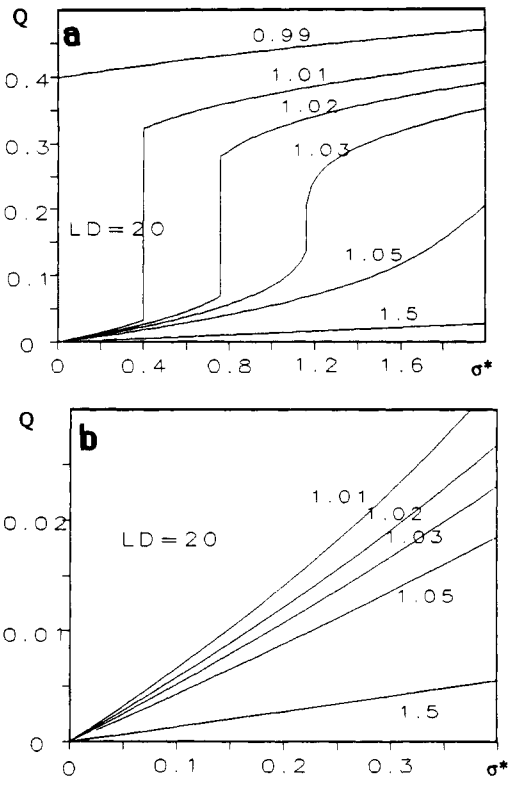

Figure 5. Order parameter Q or equivalently the stress-optical birefringence Δn in units of $\Delta\alpha$ as a function of stress σ^* for strand lengths LD = 20, where (b) is the magnifications of (a). $\Delta\alpha$ is the anisotropy in the polarizability, $\alpha_l - \alpha_t$, per unit volume in the molecular frame with α_l and α_t the parallel and perpendicular components. The curves are drawn for reduced temperatures T/T_{ni} = 0.99, 1.01, 1.02, 1.03, 1.05, and 1.5.

in our earlier work.[21] One could find similarities as an electric or magnetic field is applied to nematogenic networks instead of mechanical stress.

The birefringence of the network is given by $\Delta n = Q\Delta\alpha$, where $\Delta\alpha$ is the anisotropy in polarizability in the molecular frame divided by the monomer volume. This ignores local field corrections. Since Δn and Q are proportional, Figure 5 is also a measure of the stress-optical response. As one might expect for a system about to jump to a state of high order, the dependence of Q (or Δn) on σ^* does not remain linear for a very large region of σ^* before the discontinuities in Q. There are quadratic corrections in Figure 5b to the linear stress-optical law expected for classical elastomers (see Treloar[23] and Doi and Edwards[24] for freely jointed and Gaussian chain results, respectively). Schätzle et al.[3] find experimentally large deviations away from linearity for paranematic elastomers, a state where the perturbation analysis of our theoretical results can be used to estimate the coefficient of σ^{*2} (see section 4).

Parts a–c of Figure 6 give σ^* vs λ. Inspection of the figure shows the highly nonlinear and even discontinuous behavior one would expect for a network that is about to change shape spontaneously. A range of temperatures (reduced by the stress-free transition temperature) from 0.99 to 1.5 are plotted. For $T_{red} < 1$, there is no transition and at zero stress there is an extension λ_m we have discussed above. For T_{red} = 1.01 and 1.02, stress induces a transition and λ increases discontinuously without a further increase of σ^*. T_{red} = 1.03 is about the critical temperature for chains of length LD = 500 and a point of inflection is seen. For LD = 20 the critical temperature is higher. The increase in the magnitude of effects as LD decreases is seen by the greater curvature of the 1.05 curve in this

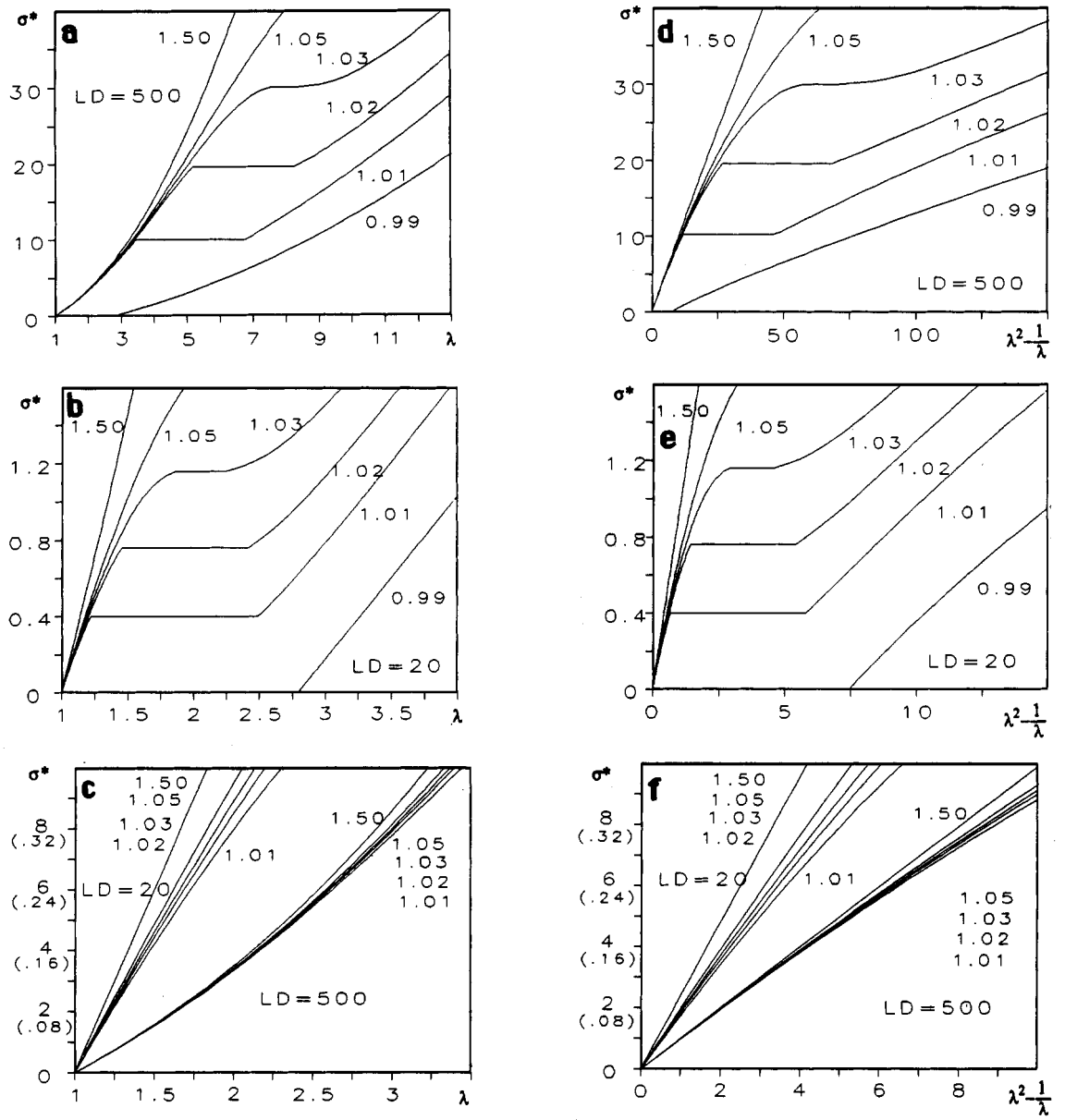

Figure 6. Stress σ^* as a function of extension λ for LD = 500 (a) and 20 (b) and (c) the magnification of small σ^* in the range λ = 1 of (a) and (b). In (c) the curves for LD = 20 are expanded by a factor of 6 with respect to the value at λ = 1 in the y axis and by a factor of 25 in the x axis. Stress σ^* as a function of $(\lambda^2 - 1/\lambda)$ is shown for LD = 500 (d) and 20 (e), and (f) shows the magnification of (d) and (e), where the curves for LD = 20 are expanded by a factor of 10 in the y axis and of 25 in the x axis. All the curves correspond to reduced temperatures T/T_{ni} = 0.99, 1.01, 1.02, 1.03, 1.05, and 1.5.

case—it is not so far away in temperature from the critical curve as 1.05 is in the LD = 500 case. The usual trend of networks with long chain length between cross-links being more compliant is followed here when the scales of the LD = 500 and 20 plots are compared.

Also interesting is the curvatures of the LD = 500 and 20 curves for small λ. They are opposite in the two cases, and Figure 6c expands this part of these two curves to bring out this point. In each case these are plotted to the value of σ^* where the discontinuity in the T_{red} = 1.01 curve is induced. These can be brought to the same scale by plotting against $\sigma^* LD$, which is the stress energy per monomer in units of $k_B T$. The λ scales are different.

Parts d–f of Figure 6 plot the same results σ^* but now against $\lambda^2 - 1/\lambda$, which for a classical rubber should be a straight line. As expected for a nematogenic network, the results, except for the very high temperature result T_{red} = 1.5, are anything but classical. Plotted this way the curvatures are the same sign.

The slopes $d\sigma^*/d\lambda$ of Figure 6, associated with the modulus $\mu = d\sigma/d \ln(\lambda)$ of the rubber, are shown in Figure 7. In contrast to the classical value which is 3 at $\sigma^* = 0$ and $\lambda = 1$ and increases monotonically, these systems have a minimum; i.e., there is a softening associated with a system that has nematic tendencies. The intercept is no longer 3, to which we return below. The effects are more pronounced as T_{red} approaches 1 as one would expect. For a temperature greater than the transition temperature, increasing stress induces an extension, i.e., a paranematic phase (see the T_{red} = 1.02 curve). When the stress reaches the critical value, the nematic–paranematic phase transition occurs; the network suddenly stretches greatly because its chains adopt their anisotropic shape. Thus, a discontinuity of λ vs σ^* appears; otherwise, we see a strong nonlinearity of the curves. In the nematic phase, the slope of the curve of λ vs σ^* around the transition is about 3 times that in the paranematic phase and the classical network (see Figure 7, T_{red} = 0.99). The shape

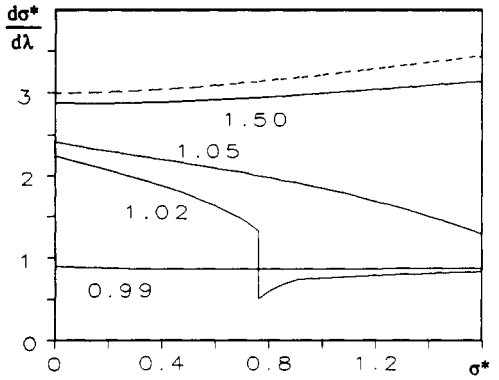

Figure 7. Derivative of σ^* with respect to extension λ as a function of stress σ^* for $LD = 20$. The curves correspond to reduced temperatures $T/T_{ni} = 0.99$, 1.02, 1.05, and 1.5. The behavior of a classical network is also shown (dashed line).

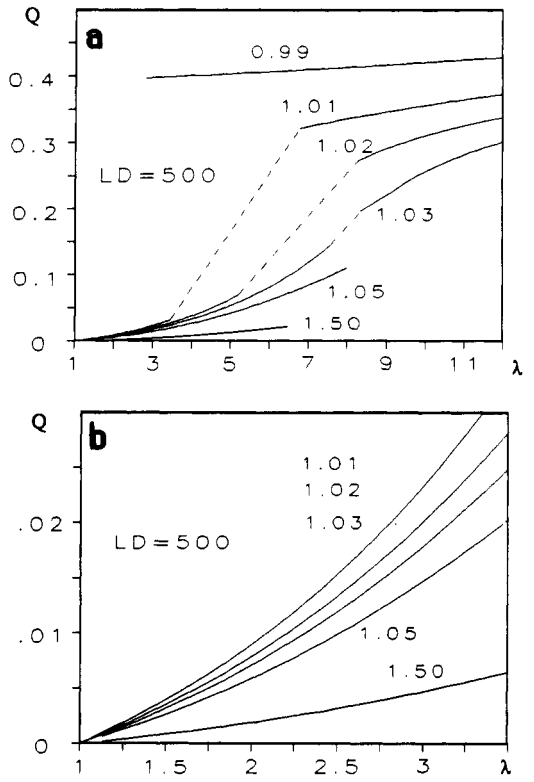

Figure 8. Order parameter Q as a function of extension λ for $LD = 500$. (b) is the magnification of (a) in an area around $\lambda = 1$. The dashed lines connect points of opposite sides of a discontinuity.

of the curve is qualitatively consistent with Schätzle et al.'s experiments for nematic phase (their Figure 3). Most remarkable are the deviations expected even for systems at $T_{red} = 1.5$ a long distance from the N–I transition, i.e., what one might term a "conventional" elastomer. We return to this in Figure 9 below.

Following Schätzle et al.[3] Figure 8 displays Q vs λ. Both are discontinuous so that as λ is increased (by application of σ^*), there comes a point where both jump, and hence this choice of plot has curious oblique discontinuities.

Deviations from classical elasticity are conventionally[25,26] displayed by plotting the so-called reduced force $\sigma^*/(\lambda^2 - 1/\lambda)$ against $1/\lambda$ (where we have further reduced σ to σ^*). Gottlieb and Gaylord[27] use this plot in a comprehensive confrontation of theory with experiment. Figure 9 shows reduced force over a range of extensions ($1/\lambda < 1$) and compressions ($1/\lambda > 1$). One sees that the shape of the curve qualitatively follows that of experiments[25,26]

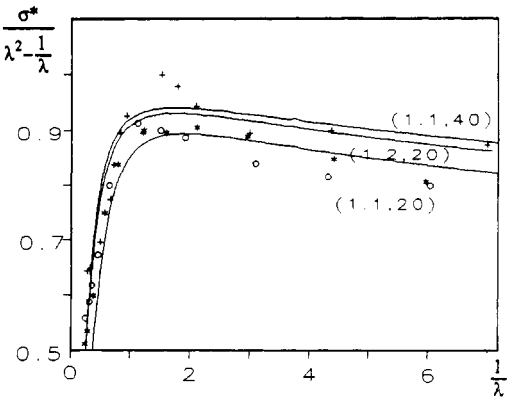

Figure 9. Dependence of reduced force $[\sigma^*/(\lambda^2 - 1/\lambda)]$ on $1/\lambda$ in extension–compression. The brackets $(T/T_{ni}, LD)$ denote the reduced temperature and strand length. They are compared with the experimental data of Pak and Flory[25] in asterisks for PDMS mixed with 3% DCP and in crosses for PDMS mixed with 2% DCP and of Rivlin and Saunders[26] in circles for natural rubber.

and offers (in the manner of Deloche and Samulski[11]) an alternative to entanglement explanations of deviation away from classical behavior, i.e., an explanation with residual nematic interactions at its root. Note that these effects are being proposed for temperatures of T_{red} around 1.2, i.e., where we are 80 K or more above any nematic transition). For the more flexible polymers of conventional elastomers any hidden (by a glass transition) nematic transition is presumably of this order away from ambient conditions. Nematic interaction is also the hypothesis of Khokhlov et al.,[5] who discuss the relative effectiveness of entanglements.[5a]

4. Perturbative Approach and Conventional Elastomers

It is most informative to develop perturbatively the theory of section 2. A central result for classical networks is the stress–optical law,[23,24] where linearity is expected between stress and birefringence. For a system about to spontaneously form a macroscopically birefringent state without the aid of applied stress, there are strong deviations from linearity. Inspection of Figure 1 (identifying Q with Δn) shows this immediately. At a fixed temperature, Q rapidly increases with σ^*, experiencing a discontinuity if $T < T_c$. Schätzle et al.'s experiments[3] on nematogenic networks found strong deviation from linearity near T_{ni}. We describe this below and find a term of the form $+\sigma^{*2}/A^3$, where A (from eq 9) gets very small near T_{ni}.

The other motive for expanding our previous expressions is the interest in residual nematic effects in conventional networks causing deviations away from classical behavior. The previous section shows a reduction of modulus and a softening with respect to classical theory. Analysis relates the extent of this to the nematic coupling in the problem.

There are several small quantities in the problem, Q, σ^*, $\lambda - 1$ and D^{-1}/L, and several systematic ways to expand. We choose a method below to get $Q(\sigma^*)$. It yields $\lambda(\sigma^*)$ rather than $\sigma^*(\lambda)$, but the former is sufficient to estimate changes in modulus.

Recall that the general distortion $\lambda(\sigma^*,Q)$ can be expressed in terms of the stress-free spontaneous distortion $\lambda_m(Q)$ appropriate to that temperature. For small σ^* the ratio $t = \lambda(\sigma^*,Q)/\lambda_m(Q)$ will be close to 1. By use of the perturbation expansion for l_z and l_p in the second approximation, λ_m is

$$\lambda_m = 1 + \frac{a}{2}Q + \frac{b}{3}Q^2 + O(Q^3) \qquad (25)$$

and W used below is

$$W = \left(\frac{l_0^3}{l_z l_p^2}\right)^{1/3} = 1 + \left(\frac{a^2}{4} - \frac{b}{3}\right)Q^2 + O(Q^3) \quad (26)$$

The cubic eq 17 gives for small σ^*/W

$$t = 1 + \frac{\sigma^*}{3W} + \frac{1}{3}\left(\frac{\sigma^*}{3W}\right)^3 + O\left\{\left(\frac{\sigma^*}{3W}\right)^4\right\} \quad (27)$$

Inserting W into t and t and λ_m back into the definition of $\lambda = \lambda_m t$, we obtain $\lambda(Q,\sigma^*)$ as

$$\lambda(Q,\sigma^*) = 1 + \left(\frac{\sigma^*}{3} + \frac{\sigma^{*3}}{81}\right) + \frac{a(3+\sigma^*)}{6}Q + \left(\frac{b}{3} + \frac{2b}{9}\sigma^* - \frac{a^2}{12}\sigma^{*2}\right)Q^2 + O(Q^3) \quad (28)$$

To obtain another connection $Q(\lambda,\sigma^*)$, one minimizes the total free energy per persistence length, F/LD, with respect to Q at fixed λ, eq 20:

$$\frac{1}{LDk_BT}\left(\frac{\partial F}{\partial Q}\right)_\lambda = AQ - BQ^2 + \frac{1}{2LD}\left[\lambda^2\frac{d}{dQ}\left(\frac{l_0}{l_z}\right) + \frac{2}{\lambda}\frac{d}{dQ}\left(\frac{l_0}{l_p}\right) - 3\frac{d}{dQ}(\ln W)\right] = 0 \quad (29)$$

As with classical elastomers, the changes in free energy due to enforced changes away from the natural shape of a chain (the λ terms) are small, being weighted by $1/LD$. Inserting $\lambda(Q,\sigma^*)$ from (28) eliminates λ, and the resultant $Q(\sigma^*)$ is

$$Q = \frac{a}{2ALD}\sigma^* + \frac{a}{24A^3(LD)^2}(6aB - 3a^2A + 8bA)\sigma^{*2} \quad (30)$$

The stress–optical law (30) reduces to the classical form for vanishing nematic influences $v_b \to 0$ and hence $\tilde{T} = k_BT/(v_b\epsilon)^{1/2} \to \infty$. In that limit $A \to 2/\tilde{T}^2$ and $a = 2/(3\tilde{T}^2)$ in (7), whence $Q = \sigma^*/(6LD) = \sigma v_p/(6k_BT)$, the factors of L dropping out since $N_s \propto 1/L$ and the classical result obtains.

Near $\tilde{T}^*$ A has a critical temperature variation, $A = 2(\tilde{T}^2 - \tilde{T}^{*2})/\tilde{T}^4$. In the numerator of the coefficient of σ^{*2} the first term (in B) dominates as A becomes small. Putting in a, A, B, (30) becomes

$$Q = \frac{\tilde{T}^2}{6\tau LD}\sigma^* + \frac{\tilde{T}^2}{1890\tau^3(LD)^2}\sigma^{*2} \equiv \frac{\tilde{T}^2}{6\tau}\left(\frac{\sigma v_p}{k_BT}\right) + \frac{\tilde{T}^2}{1890\tau^3}\left(\frac{\sigma v_p}{k_BT}\right)^2 \quad (31)$$

where $\tau = \tilde{T}^2 - \tilde{T}^{*2}$ becomes small as $\tilde{T} \to \tilde{T}_{ni}$. Its variation dominates over the less sensitive $\tilde{T}$ factors. The coefficient of the linear response is thus large as $T \to T^*$; i.e., it is proportional to $[1 - (\tilde{T}/\tilde{T}^*)^2]^{-1}(\sigma/k_BT)$ while the upward curvature $+\sigma^{*2}$ also gets very large. The response at both orders is independent of LD, the number of persistence lengths per strand, since powers of σ^*/LD are involved. A prediction of (31) is that if we write it as $Q = c_1\sigma + c_2\sigma^2$, then when τ is small and c_1 and c_2 are rapidly varying, then $c_1/c_2^3 = \text{const}$.

Relation (30) for $Q - \sigma^*$ is similar to those obtained by phenomenological calculations (see eq 8 of ref 10 and eq 12 of ref 9). Both these references obtain corrections in σ^2, though of a rather different structure since they are expressed in terms of $(\lambda^2 - 1/\lambda)$ and λ^2 instead. Neither take the form (31) since the authors were not concerned with a nearby nematic phase where B terms are probably larger than A terms in (30). They accordingly do not obtain the $1/\tau^3$ scaling for the σ^{*2} term close to the transition.

To find $\lambda(\sigma^*)$, reverse the procedure by returning to eq 28 for $\lambda(Q,\sigma^*)$ and insert $Q(\sigma^*)$:

$$\lambda(\sigma^*) = 1 + \left(\frac{1}{3} + \frac{a^2}{4ALD}\right)\sigma^* + \frac{a^2}{48A^3(LD)^2}(4A^2LD + 6aB - 3a^2A + 12bA)\sigma^{*2} \quad (32)$$

The coefficients are simple functions of temperature and strand length, whence

$$\lambda(\sigma^*) = 1 + \left(\frac{1}{3} + \frac{1}{18\tau LD}\right)\sigma^* + \frac{2 + 49\tau + 210\tau^2LD}{11340\tau^3(LD)^2}\sigma^{*2} \quad (33)$$

For a classical rubber $\lambda^2 - 1/\lambda$ is simply σ^*, but here it is

$$\lambda^2 - \frac{1}{\lambda} = \left(1 + \frac{1}{6\tau LD}\right)\sigma^* + \frac{2 + 49\tau + 210\tau^2LD}{3780\tau^3(LD)^2}\sigma^{*2} \quad (34)$$

The extension away from $\lambda = 1$ of a classical network under applied stress is given by the first term in the first set of parentheses of eq 28, setting $Q = 0$. For nematic networks some differences are found immediately: there is a new contribution to the slope $d\sigma^*/d\lambda$ at $\lambda = 1$, a reduction from the classical value 3 of $-1/(2\tau LD)$ which depends critically on how close T is to T^* (see Figure 7 at $\lambda = 1$). The slope changing with $(\tilde{T} - \tilde{T}^*)$ is clearly seen in Figure 6c, 6f.

Phenomenological approaches[9-11] arrive at this type of stress–strain relation as well. For instance, the amended coefficient of σ^* and the σ^{*2} addition to the classical σ^* term are both corrections of $O(1/N)$ or smaller than the σ^* term itself. This has been the basis of the assertion[9] that residual nematic effects cannot enter into the elasticity of conventional networks. This assertion appears to contradict numerical results shown in Figure 9, where considerable reductions in the reduced force are predicted. It is instructive to take some concrete values. Rearranging, one obtains $\tau \geq 2\tilde{T}^*(\tilde{T} - \tilde{T}^*) \sim 2\tilde{T}_{ni}(\tilde{T} - \tilde{T}_{ni}) \sim 2\tilde{T}_{ni}^2(T/T_{ni} - 1) \approx 0.3(T_{red} - 1)$, for $T > T_{ni}$. If $(T - T_{red}) \sim 70$ K and $T_{ni} = 400$ K, temperatures considerably above any fictious nematic transition, then $\tau \approx 0.05$. In our picture a conventional network is one in which the glass transition intervenes before any nematic ordering can take place. For the case of $LD \sim 20$ the addition to the coefficient of σ^* in (34) is $\sim 16\%$. Taking the last term of the coefficient of σ^{*2}, the ratio of the σ^* to σ^{*2} terms is $\sigma^*/18\tau LD$, i.e., $\sim 20\%$ at $\lambda = 2$. These crude estimates are of the order seen from the full numerical solution (Figure 9) and indicate that nematic effects could be expected to be significant in conventional elastomers. For the above case of τ and LD the three terms in (34) for σ^{*2} are roughly in the ratio 2:2.5:10; i.e., the above was an underestimate for the importance of the σ^{*2} term. Of more significance, when these terms are of similar size, then the LD dependence of the deviations from classical will no longer be cleanly $1/LD$. It has been suggested experimentally[28] that indeed the $Q - (\lambda^2 - 1/\lambda)$ relation does not have a simple $1/LD$ dependence.

The proposal that a significant part of the elastic response of a conventional network arises from *nematic* causes suggests that it may be profitable to reanalyze the results of thermodynamic investigations of networks (see, for instance, Ciferri et al.[29]). This and later work were concerned with how much of the stress is nonentropic in origin; for instance, how intrachain interactions give a temperature dependence to chain dimensions and hence an energetic component to stress. These considerations[29] do

not change the underlying $(\lambda^2 + 2/\lambda)$ form. This is in contrast to our work, which is concerned with nematic interchain energetic effects. Since chain shape (anisotropy) is thereby changed, this additional term is not of the form $(\lambda^2 + 2/\lambda)$ and there is a shift on the reduced force vs $1/\lambda$ plot.

5. Conclusions

The properties of nematic elastomers depend on the coupling between mechanical stress and nematic order. The coupling is mediated by chains that can equally change their shape by responding to external stress or to nematic energetic influences. Evaluating chain shape as a function of nematic order and putting these expressions into a theory of the elasticity of anisotropic Gaussian chains describe a wide range of phase and mechanical properties.

In addition to describing these new elastomers, we find that, in accord with Deloche and Samulski[11] and Abramchuk and Khokhlov,[5] residual nematic interactions cause deviations away from classical behavior even in "conventional" elastomers. Conventional networks are the high-temperature phases of our nematic networks. Qualitative agreement is achieved with stress–strain experiments.

References and Notes

(1) de Gennes, P.-G. *C. R. Acad. Sci. Ser.* **1975**, *B281*, 101.
(2) de Gennes, P-G. In *Polymer Liquid Crystals*; Ciferri, A., Krigbaum, W. R., Meyer, R. B., Eds.; Academic Press: New York, 1982.
(3) Schätzle, J.; Kaufhold, W.; Finkelmann, H. *Makromol. Chem.* **1989**, *190*, 3269.
(4) Warner, M.; Gelling, K. P.; Vilgis, T. A. *J. Chem. Phys.* **1988**, *88*, 4008.
(5) (a) Abramchuk, S. S.; Khokhlov, A. R. *Dokl. Akad. Nauk SSSR* (in Russian) **1987**, *297*, 385; (Engl. Transl.) *Dokl. Phys. Chem.* **1988**, 297, 1069. Abramchuk, S. S.; Nyrkova, I. A.; Khokhlov, A. R. *Polym. Sci.* (in Russian) **1989**, *31*, 490 (b) and 1759 (c).
(6) Wang, X. J.; Warner, M. *J. Phys.* **1986**, *A19*, 2215.
(7) Anisotropic Gaussian chains have been seen in neutron scattering studies of melt conformations. Side-chain polymers by: (a) Kirste, R. G.; Ohm, H. G. *Makromol. Chem. Rapid. Commun.* **1985**, *6*, 179. Main-chain polymers by: (b) D'allest, J. F.; Sixou, P.; Blumstein, A.; Blumstein, R. B.; Teixeira, J.; Noirez, L. *Mol. Cryst. Liq. Cryst.* **1988**, *155*, 581.
(8) Tanaka, T.; Allen, G. *Macromolecules* **1977**, *10*, 426.
(9) Jarry, J. P.; Monnerie, L. *Macromolecules* **1979**, *12*, 316.
(10) Deloche, B.; Samulski, E. T. *Macromolecules* **1981**, *14*, 575.
(11) Deloche, B.; Samulski, E. T. *Macromolecules* **1988**, *21*, 3107.
(12) Wang, X. J.; Warner, M. *J. Phys.* **1987**, *A20*, 713.
(13) Legge, C. H.; Mitchell, G. R.; Davis, F. J. Presented at the 1990 Annual Conference of the British Liquid Crystal Society, Bristol, April 9–11, 1990; P16. Also to be published in *J. Phys. (Paris)*.
(14) Zentel, R.; Benalia, M. *Makromol. Chem.* **1987**, *188*, 665.
(15) Mattoussi, H.; Ober, R.; Veyssie, M.; Finkelmann, H. *Europhys. Lett.* **1986**, *2*, 233.
(16) Warner, M.; Gunn, J. M. F.; Baumgärtner, A. *J. Phys.* **1985**, *A18*, 3007.
(17) Rusakov, V. V.; Shliomis, M. I. *J. Phys. Lett.* **1985**, *46*, L935.
(18) ten Bosch, A.; Maissa, P.; Sixou, P. *Phys. Lett.* **1983**, *A94*, 298.
(19) Maier, W.; Saupe, A. *Z. Naturforsch.* **1959**, *14a*, 882. We use a potential of this form since it is the simplest that encapsulates the quadrupolar symmetry of the nematic environment; see ref 16 for a discussion.
(20) Bouwkamp, C. J. *J. Math. Phys.* **1947**, *26*, 79.
(21) Wang, X. J.; Warner, M. *Phys. Lett.* **1986**, *A119*, 181.
(22) Hornreich, R. M. *Phys. Lett.* **1985**, *A109*, 232.
(23) Treloar, L. R. G. *The Physics of Rubber Elasticity*, 3rd ed.; Clarendon Press: Oxford, U.K., 1975.
(24) Doi, M.; Edwards, S. F. *The Theory of Polymer Dynamics*; Clarendon Press: Oxford, U.K., 1986.
(25) Pak, H.; Flory, P. J. *J. Polym. Sci.* **1979**, *17*, 1845.
(26) Rivlin, R. S.; Saunders, D. W. *Philos. Trans. R. Soc. London* **1951**, *A243*, 251.
(27) Gottlieb, M.; Gaylord, R. J. *Polymer* **1983**, *24*, 1644.
(28) Dubault, A.; Deloche, B.; Herz, J. *Polymer* **1984**, *25*, 1405.
(29) Ciferri, A.; Hoeve, C. A. J.; Flory, P. J. *J. Am. Chem. Soc.* **1961**, *83*, 1015.